Available online at www.sciencedirect.com

SciVerse ScienceDirect

Ceramics International 38 (2012) 5201–5207

CERAMICS INTERNATIONAL

www.elsevier.com/locate/ceramint

Enhancement of the photocatalytic performance of Ag-modified TiO_2 photocatalyst under visible light

Cheewita Suwanchawalit [a,*], Sumpun Wongnawa [b], Pimpaporn Sriprang [b], Pachara Meanha [a]

[a] Department of Chemistry, Faculty of Science, Silpakorn University, Sanam Chandra Palace Campus, Nakornpathom 73000, Thailand
[b] Department of Chemistry, Faculty of Science, Prince of Songkla University, Hat Yai, Songkhla 90112, Thailand

Received 23 December 2011; received in revised form 24 February 2012; accepted 9 March 2012
Available online 19 March 2012

Abstract

A highly visible-light photocatalytic active Ag-modified TiO_2 (Ag–TiO_2) was prepared by a simple sol–gel process using $TiOSO_4$ as the starting material, $AgNO_3$ as a silver doping source, and hydrazine as a reducing agent. The prepared Ag–TiO_2 samples were characterized by several techniques such as X-ray powder diffraction (XRD), BET surface area measurement, scanning electron microscopy (SEM), transmission electron microscopy (TEM), inductively coupled plasma optical emission spectroscopy (ICP-OES), energy dispersive X-ray spectrometry (EDX), X-ray absorption spectroscopy (XAS) and UV–vis diffuse reflectance spectroscopy (DRS). The Ag–TiO_2 photocatalyst, a mixture of amorphous and anatase phases, has a high surface area. The silver contents in the Ag–TiO_2 samples were determined by ICP measurements. The diffused reflectance UV–vis spectra indicated that the Ag–TiO_2 samples exhibited higher red shifts compared with the undoped TiO_2 sample. Indigo carmine degradation under visible irradiation indicated that the Ag–TiO_2 catalyst gave higher photocatalytic efficiency than those of commercial P25-TiO_2 and undoped-TiO_2 samples. The Ag–TiO_2 catalyst can be reused many times without any additional treatment.
© 2012 Elsevier Ltd and Techna Group S.r.l. All rights reserved.

Keywords: A. Sol–gel process; Titanium dioxide; Mesoporous titanium dioxide; Ag-modified TiO_2; Indigo camine; Dye decolorization

1. Introduction

Heterogeneous semiconductor photocatalysis is an attractive technology among the most promising technologies for solar energy conversion and environmental applications. Of the semiconducting materials employed, TiO_2 is the most effective because of its high photosensitivity, chemical stability, non-toxicity, easy availability, environmental friendliness, and low cost [1–4].

However, a major drawback of TiO_2 is the large band gap of 3.2 eV which limits its activity when sunlight is used. To overcome these limitations of TiO_2, many studies have been carried out to enhance the electron–hole separation and to extend the absorption range of TiO_2 into the visible region. These studies involved incorporation of metal ions or nonmetal ions into the TiO_2 lattice [5–8], dye photosensitization onto the TiO_2 surface [9–12], and deposition of noble metals onto the TiO_2 surface [13–15].

In particular, noble metal-modified TiO_2 particles have become the focus of many studies to maximize the efficiency of photocatalytic reactions. The noble metals deposited or doped on TiO_2 have high Schottky barriers among the metals and act as electron traps, facilitating the electron–hole separation and promoting the interfacial electron transfer process [16]. These noble metals may enhance the electron–hole separation, extend the light absorption into the visible range and enhance the surface electron excitation.

Among the noble metals used as electron traps, silver (Ag) is extremely suitable for industrial application due to its low cost and easy preparation. Ag-modified TiO_2 powders have become current interests due to its improvement of photocatalytic reactions and anti-microbial activity. There are several techniques for the preparation of Ag-modified TiO_2 such as sol–gel [16,17], photocatalytic deposition [13], and deposition precipitation [14].

In this work, undoped and Ag-modified TiO_2 samples were synthesized by the sol–gel process using $TiOSO_4$ and $AgNO_3$ as starting materials and hydrazine as a reducing agent. Herein, the synthesized Ag-modified TiO_2 catalyst was characterized

* Corresponding author. Tel.: +66 3425 5797; fax: +66 3427 1356.
E-mail addresses: cheewita@su.ac.th, cheewita_31@hotmail.com (C. Suwanchawalit).

0272-8842/$36.00 © 2012 Elsevier Ltd and Techna Group S.r.l. All rights reserved.
doi:10.1016/j.ceramint.2012.03.027

by various physical techniques such as XRD, SEM, TEM, BET, DRS, EDX, ICP-OES and XAS techniques. The photocatalytic activity of the prepared catalysts was determined using indigo carmine as a model pollutant and the results compared with that of commercial Degussa P25-TiO_2 under visible irradiations.

2. Experimental

2.1. Synthesis of undoped-TiO_2 and Ag-modified TiO_2 catalysts

The undoped-TiO_2 was prepared by the sol–gel method. A 0.5 M $TiOSO_4$ aqueous solution was refluxed at 90 °C and then ammonia solution was added until the pH was 7 and then refluxed at 90 °C for 24 h to give TiO_2 precipitates. This precipitates were washed several times and dried at 105 °C for a day to give the undoped-TiO_2 powders.

In a typical preparation of Ag-modified TiO_2 catalyst, a 0.5 M $TiOSO_4$ aqueous solution was refluxed at 90 °C and then concentrated ammonia solution was added to the $TiOSO_4$ solution until the pH was 7. A 5.0 mmol% silver nitrate solution was added to the mixture followed by a 10.0 mmol% hydrazine solution and the mixture was refluxed at the same temperature for 24 h to give Ag–TiO_2 precipitates. The Ag–TiO_2 precipitates were washed several times until free of sulfate ion by the $BaCl_2$ solution test. The washed Ag–TiO_2 sample was dried at 105 °C for a day to give the Ag–TiO_2 catalyst.

2.2. Characterization of the catalysts

X-ray diffraction (XRD) patterns of the samples were recorded on a Rigaku MiniFlex II X-Ray diffractometer with Cu K_α radiation (0.15406 nm) from 20° to 80° (2θ) to assess the crystallinity of the catalysts. The specific surface area and pore size distribution of the TiO_2 samples were determined by analyzing the N_2 adsorption isotherms obtained at 77 K using a Belsorp-Max automatic specific surface area analyzer. The particle morphologies were investigated using a scanning electron microscope (Quanta400) and transmission electron microscope (JEOL JSM 2010). The energy dispersive X-ray spectrometry technique (ISIS 300) was used to determine all elements in the samples. The Ag content was measured on a Perkin Elmer Optima 4300DV ICP-OES. Ag *L*3-edge XANES measurements were carried out using double crystal monochromator InSb (1 1 1) in the fluorescent mode with a 13-component Ge detector (Canbera) at the X-ray absorption spectroscopy beamline (BL-8) of the Siam Photon, National Synchrotron Research Center, Nakhon Ratchasima, Thailand. The band gap energies were determined using a Shimadzu UV-2401 spectrophotometer. The spectra were recorded in the diffused reflectance mode with $BaSO_4$ as a reference.

2.3. Evaluation of the photocatalytic activity of the Ag-modified TiO_2 catalysts

The experiments were performed by using 0.05 g TiO_2 sample dispersed in 50 mL of Indigo carmine (IC) solution. Prior to illumination, the suspension was stirred for 1 h to allow the adsorption equilibrium of the dye onto the surface of the TiO_2 sample. Then the mixture was irradiated under visible light irradiation (using a 18 W fluorescence TL-D 18 W/865 Philips tubelight as a visible light source). In all studies, the mixture was magnetically stirred during illumination. At given irradiation time intervals, samples were collected and centrifuged to separate TiO_2 powders. The residual concentration of IC was monitored by the change in absorbance of the dye at 610 nm using a UV-Vis spectrophotometer. Similar measurements were carried out on commercial P25-TiO_2. Controlled experiments either without light or TiO_2 were performed to ensure that degradation of the dye was dependent on the presence of both light and TiO_2. The disappearance of IC was analyzed by a Specord S100 UV–Vis spectrophotometer (Analytik Jena GmbH) over the 200–800 nm range.

3. Results and discussion

3.1. Characterization of the Ag-modified TiO_2

The XRD patterns of the undoped TiO_2 and the as-synthesized Ag–TiO_2 at different Ag contents are shown in Fig. 1 which all the synthesized Ag–TiO_2 and the undoped TiO_2 exist in the anatase phase. The peaks located at 25.4, 37.8, 48.0, 54.2, 62.7, 69.5, 75.2° respond to the reflections from the (1 0 1), (0 0 4), (2 0 0), (1 0 5), (2 0 4), (2 2 0) and (2 1 5) planes of the anatase phase (JCPDS No. 21-1272). The average crystallite sizes of anatase in the samples were calculated by applying the Debye–Scherrer formula,

$$D = \frac{\kappa\lambda}{\beta\cos\theta} \quad (1)$$

where D is the average crystallite size in angstroms, κ is a constant which is usually taken as 0.89, λ is the wavelength of

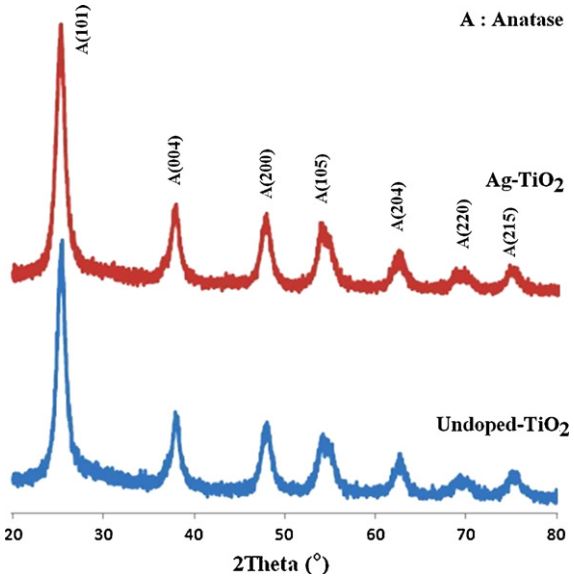

Fig. 1. XRD patterns of the undoped TiO_2 and prepared Ag-modified TiO_2 catalysts.

Table 1
The crystallite size, surface area, and band gap energy of Ag–TiO_2 samples.

Ag–TiO_2 samples	Crystallite size (nm)	Surface area (m^2/g)	Band gap energy (eV)
Undoped-TiO_2	7.3	200	3.19
Ag–TiO_2	6.8	256	3.08

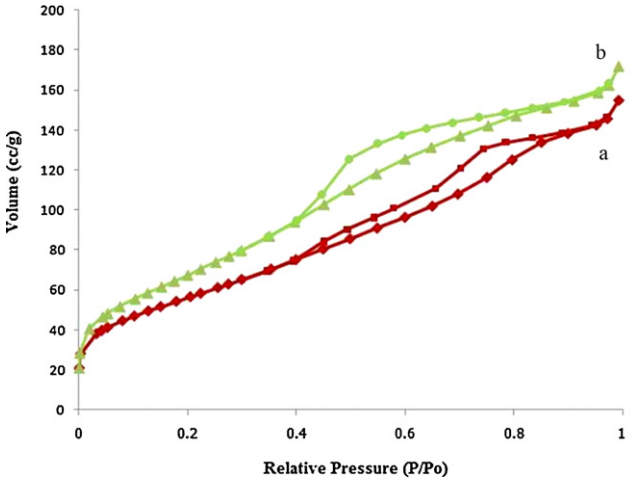

Fig. 2. N_2-adsorption–desorption isotherm of the undoped TiO_2 (a) and the prepared Ag-modified TiO_2 catalysts (b).

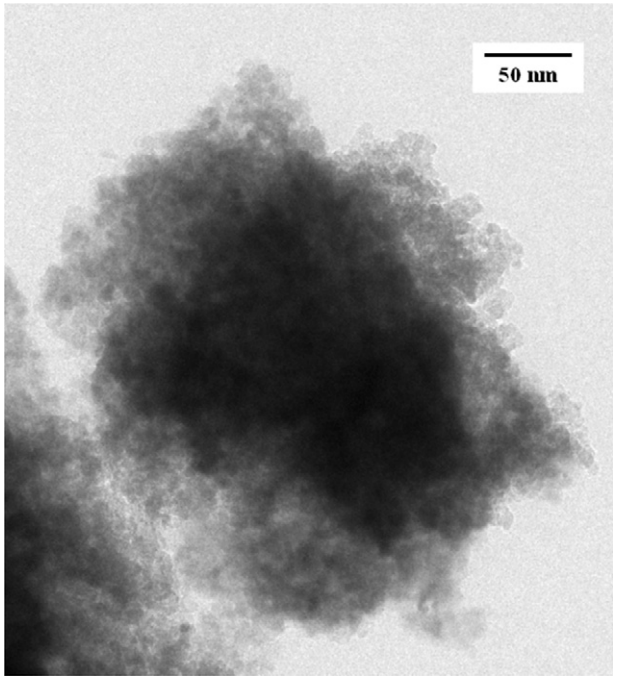

Fig. 3. TEM images of Ag–TiO_2 samples at magnification ×40,000.

the X-ray radiation (Cu K_α = 0.15406 nm), β is the corrected band broadening (full width at half-maximum (FWHM)), and θ is the diffraction angle. The phase structure and average crystallite size of the TiO_2 samples are given in Table 1. However, no obvious diffraction peaks of Ag are found, which can be attributed to the low doping Ag content (5 mmol%). The anatase peak of Ag–TiO_2 is slightly broad which is an indication that the products are not well-grown crystalline since they were not calcined. Therefore, an amorphous form must be present in these samples. The degrees of anatase crystallinity present in the samples were determined from the XRD intensities by using the standard addition method as previously described [18,19]. The Ag–TiO_2 sample contains 28.4% anatase phase with the rest in amorphous form (71.6%) while the undoped TiO_2 sample contains 27.5% anatase and 72.5% of an amorphous.

The nitrogen adsorption–desorption isotherms of the samples (Fig. 2) appear to be of the type IV (BDDT classification), indicating that the mesoporous structure was formed. The specific surface areas of the undoped TiO_2 and Ag–TiO_2 are given in Table 1. The results revealed that Ag-modified TiO_2 had a higher specific surface area than that of pure TiO_2. In addition, the TEM results (Fig. 3) were consistent with the mesoporous structure appearing between the aggregated anatase crystals.

The surface microstructures of the synthesized Ag–TiO_2 was investigated by SEM (Fig. 4) and TEM techniques. Both SEM

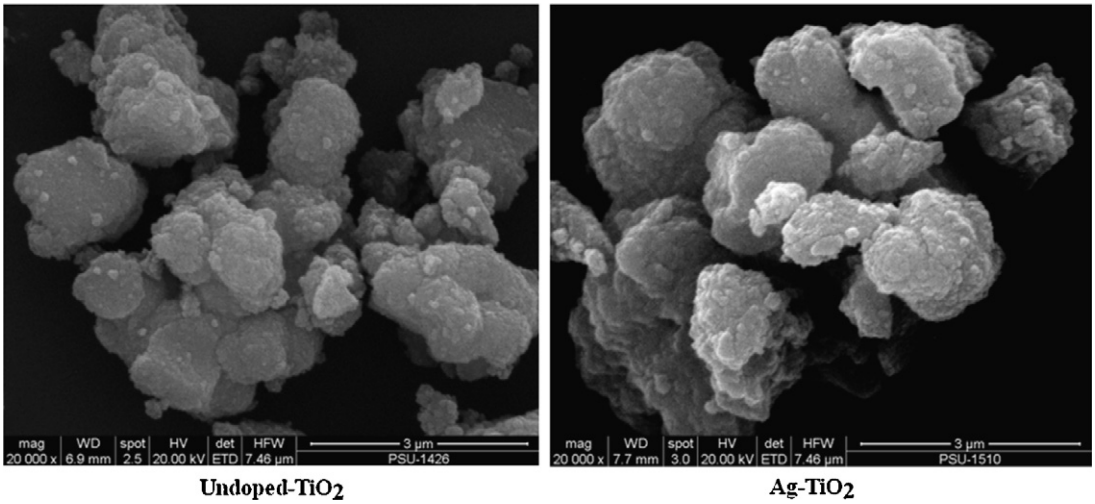

Undoped-TiO_2 Ag-TiO_2

Fig. 4. SEM images of undoped TiO_2 and Ag–TiO_2 catalysts.

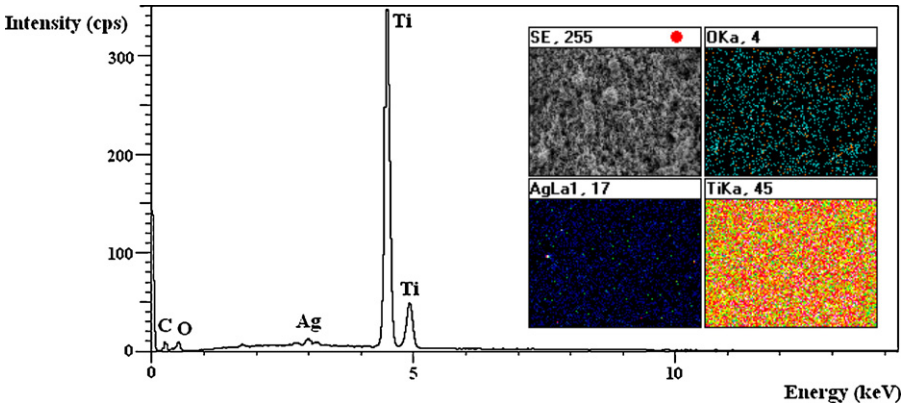

Fig. 5. EDX spectra of Ag–TiO_2 sample and the elemental mapping mode (inset).

and TEM images showed high degree of aggregation of some anatase crystals. From TEM image, it is evident that the particle size agrees well with the crystallite size determined from XRD measurement. The estimated crystallite size from the TEM technique (comparing the size with the scale bar in TEM image) is *ca.* 6–9 nm corresponding with XRD results. The silver particles could not be observed by SEM and TEM due to the smaller size of Ag particles coated on the surface of TiO_2. However, the presence of silver could be investigated by EDX, ICP and XAS techniques. The EDX mapping of Ag–TiO_2 sample is illustrated in Fig. 5 (inset). From elemental mapping mode highly and uniformly dispersed Ag particles on the TiO_2 support were observed. The Ag content loaded on the porous TiO_2 was determined by ICP-OES measurement. For this work, 5 mmol% Ag was loaded onto the TiO_2 surface. The ICP-OES results (5.42 mmol%Ag) suggest that the estimated silver content is in good agreement with the expected theoretical values.

The diffuse reflectance spectra (DRS) were used to estimate the band gap energy and optical property of sample. The DRS spectra of undoped TiO_2 and prepared Ag–TiO_2 catalysts are illustrated in Fig. 6. The strong broad band from 200 to 380 nm can be ascribed to the charge-transfer absorption from the valence band (2p orbital of the oxide anions) to the conduction band (3d orbital of the Ti^{4+}cations) within the solid [20]. The addition of silver particles causes significant changes to the absorption spectra of TiO_2 in the visible region which is characteristic of surface plasmon absorption. The absorption edge is obtained by the linear extrapolation of the steep part of the UV adsorption toward the baseline. The band gap energies are calculated from Eq. (2) and are shown in Table 1.

$$E_g = h\frac{C}{\lambda} \tag{2}$$

where E_g is the band gap energy (eV), h is the Planck's constant, c is the light velocity (m/s), and λ is the wavelength (nm). These band gaps of all Ag–TiO_2 catalysts slightly shift to higher wavelength indicating that lower energy transitions are possible. The spectra reveal that Ag doping has a marked effect on the absorption of light in the visible region by TiO_2 to be increased with an increase in the silver content. The absorption edge shifts towards longer wavelengths for the Ag–TiO_2 catalysts, indicating a decrease in the band gap energies of TiO_2 with increasing amount of silver.

The chemical state of Ag was characterized by XANES (X-Ray Near Edge Structure) technique (Fig. 7). Ag L3-edge XANES was used to identify the form of Ag in Ag-modified TiO_2 sample. The results showed that Ag^+ ion should be in the

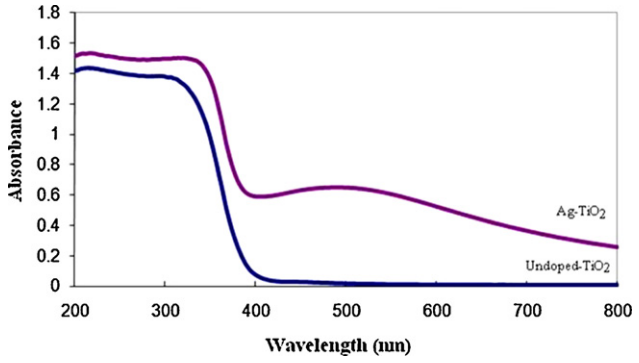

Fig. 6. DRS spectra of undoped TiO_2 and as-synthesized Ag–TiO_2 catalysts.

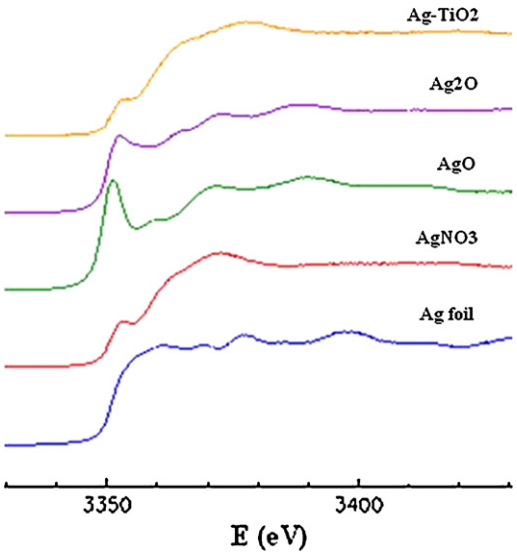

Fig. 7. Ag L3-edge of XANES of 5Ag–TiO_2.

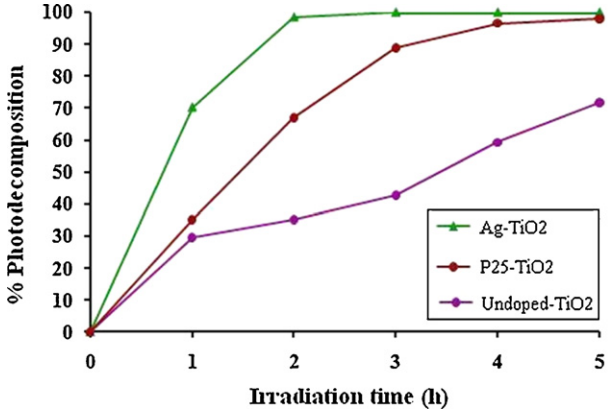

Fig. 8. Photocatalytic activity of Ag–TiO_2 samples under visible light irradiation.

free form as Ag+ in $AgNO_3$ as the fingerprint (Ag L3-edge XANES) analysis.

3.2. Photocatalytic activity

Indigo carmine (IC) was employed in this study to assess the photocatalytic activity of the as-prepared titania samples. The commercial reference material, Degussa P25-TiO_2, was used to compare the efficiency of decolorization of the IC solution with the prepared Ag–TiO_2 samples and the undoped TiO_2 sample. The amount of catalyst was 1.0 g/L (or 0.05 g in 50 mL) and the dye concentration was 2.5×10^{-5} M. The efficiency of decolorization of the IC solution with the prepared TiO_2 catalysts under visible irradiation is shown in Fig. 8. It could be explained that the Ag particles deposited on the TiO_2 surface can act as electron–hole separation centers [13,20,21]. The electron transfer from the TiO_2 conduction band to metallic silver particles at the interface is thermodynamically possible because the Fermi level of TiO_2 is higher than that of the silver metals. This causes the formation of the Schottky barrier at Ag-modified TiO_2 contact region which improves the charge separation and thus enhances the photocatalytic activity of TiO_2. Under visible irradiation, IC is activated into its excited state, injecting an electron into the conduction of TiO_2. The injected electron on the TiO_2 particle reacts with adsorbed O_2 to produced active oxygen radicals. In this mechanism, the TiO_2 acts only as an electron-transfer and the oxygen as an electron acceptor. The Ag particles on the TiO_2 surface can act as electron traps enhancing the electron–hole separation.

The proposed photocatalytic degradation mechanisms of indigo carmine using Ag-modified TiO_2 as photocatalyst as following equations;

$$\mathrm{Ag{-}TiO_2} + h\nu \rightarrow \mathrm{Ag{-}TiO_2(e_{CB}^-)} + \mathrm{Ag{-}TiO_2(h_{VB}^+)} \quad (3)$$

$$\mathrm{IC} + h\nu \rightarrow \mathrm{IC^*} \quad (4)$$

$$\mathrm{IC^*} + \mathrm{Ag{-}TiO_2} \rightarrow \mathrm{IC^+} + \mathrm{Ag{-}TiO_2(e_{CB}^-)} \quad (5)$$

$$(\mathrm{O_2})_{ads} + \mathrm{Ag{-}TiO_2(e_{CB}^-)} \rightarrow \mathrm{O_2^{\bullet -}} \quad (6)$$

$$(\mathrm{H_2O} \leftrightarrow \mathrm{H^+ + OH^-})_{ads} + \mathrm{Ag{-}TiO_2(h_{VB}^+)} \rightarrow \mathrm{H^+ + OH^\bullet} \quad (7)$$

$$\mathrm{O_2^{\bullet -} + H^+} \rightarrow \mathrm{HO_2^\bullet} \quad (8)$$

$$\mathrm{2HO_2^\bullet} \rightarrow \mathrm{H_2O_2 + O_2} \quad (9)$$

$$\mathrm{H_2O_2 + e^-} \rightarrow \mathrm{OH^\bullet + OH^-} \quad (10)$$

$$\mathrm{IC + OH^\bullet} \rightarrow \mathrm{IC^\bullet + H_2O} \quad (11)$$

$$\mathrm{IC + Ag{-}TiO_2(h^+)} \rightarrow \mathrm{IC^{+\bullet}} \rightarrow \mathrm{degradationproducts} \quad (12)$$

In practical uses, the catalyst may be used in environment with varying acidities, hence, all TiO_2 catalysts were tested for their activities at various pH values. As the charge of the IC molecules and the surface of the TiO_2 photocatalyst are both pH-dependent, so the influence of pH on the degradation of dye was studied in the pH range 3–9 including the natural pH of IC solution at 6.4. The pH was adjusted by adding aqueous solution of either HCl or NaOH, respectively. The effect of pH on the adsorption of dye on the surface of the TiO_2 catalyst and the photodegradation of the dye in an aqueous TiO_2 suspension are shown in Fig. 9. It is well known that pH would influence both the surface state of titania and the ionization state of ionizable dye molecules. The points of zero charge (pzc) of the TiO_2 (Degussa P25), undoped TiO_2, and Ag-modified TiO_2 are *ca.* 6.8 [22], 6.0, and 6.0, respectively. Thus, the TiO_2 surface is positively charged in acidic media

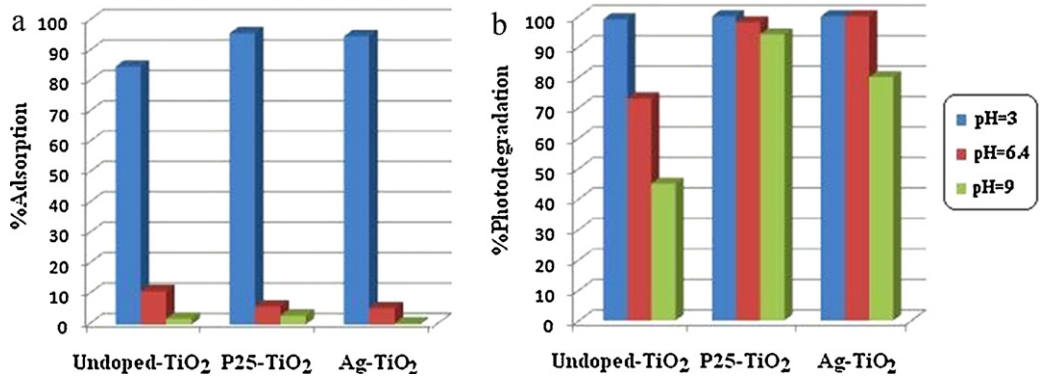

Fig. 9. Effect of pH on (a) adsorption of IC on the catalyst surface, and (b) the photocatalytic decomposition of IC. (conditions: TiO_2 1 g/L, 50 mL IC solution (a) adsorption in the dark 0.5 h, and (b) under visible light irradiation 5 h).

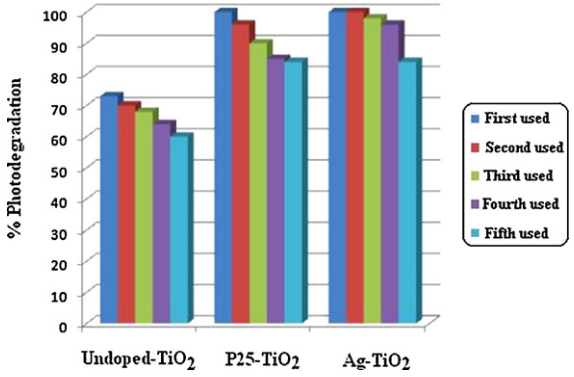

Fig. 10. The photocatalytic efficiency from recyclability test of Ag–TiO_2 under visible light irradiation of 5 h.

($pH < pH_{pzc}$), whereas it is negatively charged under alkaline condition ($pH > pH_{pzc}$) [23]. Since the parent fragment of IC bears a negative charge, the adsorption on a positively charged to surface of TiO_2 is favored at low pH. Increasing the pH caused the surface of TiO_2 become less positive or even turn to negative once the pH exceeded pH_{pzc}. Hence, we expect the repulsive force between the two negative charges of the dye parent fragment and the surface charge of the catalyst to operate more strongly at high pH, resulting in less adsorption of the dye onto the TiO_2 surface. For photocatalytic decomposition, the results are shown in Fig. 9b. The Ag-modified TiO_2 and P25-TiO_2 catalysts showed a higher decomposition rate than the undoped-TiO_2 catalyst across the pH range under investigation, indicating that these TiO_2 samples can be used in widely varied pH conditions.

The recyclability of the Ag-deposited TiO_2 photocatalysts was examined in order to check their potential use in practical systems. In this work, the used Ag-modified TiO_2 sample was separated from the suspension by gravity sedimentation and used in the next runs without any extra treatment. The Ag–TiO_2 catalyst have crystallite size in the range of 6–7 nm, but they have aggromerated to larger particle size, so they could settle to the bottom faster than Degussa P25-TiO_2 which has crystallite size of 25 nm. The reusability test was shown in Fig. 10 which reveals that the activity of the Ag-modified TiO_2 and P25-TiO_2 sample slightly decline in efficiency until the fifth use. On the other hand, for the undoped TiO_2 sample the photocatalytic activity gradually decreased until only 60% of IC was decomposed in the fifth run.

4. Conclusions

The Ag-modified TiO_2 catalyst was prepared by the sol–gel process using hydrazine as a reducing agent. The Ag-modified TiO_2 existed in the anatase phase with a high surface area of 256 m^2/g with narrow pore size distribution and had light absorption extended to the visible region. The deposited silver particles on the surface of TiO_2 was investigated by EDX, XAS, and ICP analyses. The Ag particles were found in $AgNO_3$ species as confirmed by XANES techniques. The Ag-modified TiO_2 catalyst has high photocatalytic efficiency than those of undoped TiO_2 and commercial P25-TiO_2 under visible light irradiation. Furthermore, the Ag-modified TiO_2 catalyst can be used several times without any treatment process. The simple preparation combined with its high photocatalytic activity makes it an attractive candidate for applications in the wastewater treatment industries.

Acknowledgments

This research is supported by the Faculty of Science, Silpakorn University, Thailand. We would like to thank the Synchrotron Light Research Institute (Public Organization), Nakhon Ratchasima, Thailand for XAS: XANES analysis.

References

[1] M.A. Fox, M.T. Dulay, Heterogeneous photocatalysis, Chem. Rev. 93 (1993) 341–357.
[2] O. Legrini, E. Oliveros, A.M. Braun, Photochemical processes for water treatment, Chem. Rev. 93 (1993) 671–698.
[3] M.I. Litter, Heterogeneous photocatalysis transition metal ions in photocatalytic systems, Appl. Catal. B: Environ. 23 (1999) 89–114.
[4] O. Carp, C.L. Huisman, A. Reller, Photoinduced reactivity of titanium dioxide, Prog. Solid State Chem. 32 (2004) 33–177.
[5] D. Chatterjee, S. Dasgupta, Visible light induced photocatalytic degradation of organic pollutants, J. Photochem. Photobiol. C: Photochem. Rev. 6 (2005) 186–205.
[6] A. Di Paolar, G. Marci, L. Palmisano, M. Schiavello, K. Uosaki, S. Ikeda, B. Ohtani, Preparation of polycrystalline TiO_2 photocatalysts impregnated with various transition metal ions: characterization and photocatalytic activity for the degradation of 4-nitrophenol, J. Phys. Chem. 106 (2002) 637–645.
[7] H. Yamashita, M. Honda, M. Harada, Y. Ichihashi, M. Anpo, T. Hirao, N. Itoh, N. Iwamoto, Preparation of Titanium oxide photocatalysts anchored on porous silica glass by a metal ion-implantation method and their photocatalytic reactivities for the degradation of 2-propanol diluted in water, J. Phys. Chem. B 102 (1998) 10707–10711.
[8] W. Su, Y. Zhang, Z. Li, L. Wu, X. Wang, J. Li, X. Fu, Multivalency iodine doped TiO_2: preparation, characterization, theoretical studies, and visible-light photocatalysis, Langmuir 24 (2008) 3422–3428.
[9] C. Wang, J. Li, G. Mele, G.M. Yang, F.X. Zhang, L. Palmisano, G. Vasapollo, Efficient degradation of 4-nitrophenol by using functionalized porphyrin–TiO_2 photocatalysts under visible irradiation, Appl. Catal. B: Environ. 76 (2007) 218–226.
[10] G. Mele, R.D. Sole, G. Vasapollo, E.G. Lopez, L. Palmisano, M. Schiavello, Photocatalytic degradation of 4-nitrophenol in aqueous suspension by using polycrystalline TiO_2 impregnated with functionalized Cu(II)-porphyrin or Cu(II)-phthalocyanine, J. Catal. 217 (2003) 334–342.
[11] Y. Li, M. Guo, S. Peng, G. Lu, S. Li, Formation of multilayer-Eosin Y-sensitized TiO_2 via Fe^{3+} coupling for efficient visible-light photocatalytic hydrogen evolution, Int. J. Hydrogen Energy 34 (2009) 5629–5636.
[12] V. Nguyen, J.C.S. Wu, C.H. Chiou, Photoreduction of CO_2 over Ruthenium dye-sensitized TiO_2-based catalysts under concentrated natural sunlight, Catal. Commun. 9 (2008) 2073–2076.
[13] H.M. Sung-Suh, J.R. Choi, H.J. Hah, S.M. Koo, Y.C. Bae, Comparison of Ag deposition effects on the photocatalytic activity of nanoparticulate TiO_2 under visible and UV light irradiation, J. Photochem. Photobiol. A: Chem. 163 (2004) 37–44.
[14] X. You, F. Chen, J. Zhang, M. Anpo, A novel deposition precipitation method for preparation of Ag-loaded titanium dioxide, Catal. Lett. 102 (2005) 247–250.
[15] H.Y. Chuang, D.H. Chen, Fabrication and photocatalytic activities in visible and UV light regions of Ag–TiO_2 and NiAg–TiO_2 nanoparticles, Nanotechnology 20 (2009) 1–10.

[16] M.S. Lee, S.S. Hong, M. Mohseni, Synthesis of photocatalytic nanosized TiO_2–Ag particles with sol–gel method using reduction agent, J. Mol. Catal. A: Chem. 242 (2005) 135–140.

[17] H.E. Chao, Y.U. Yun, H.U. Xingfang, A. Larbot, Effect of silver doping on the phase transformation and grain growth of sol–gel titania powder, J. Eur. Ceram. Soc. 23 (2003) 1457–1464.

[18] M. Kanna, S. Wongnawa, Mixed amorphous and nanocrystalline TiO_2 powders prepared by sol–gel method: characterization and photocatalytic study, Mater. Chem. Phys. 110 (2008) 166–175.

[19] C. Suwanchawalit, S. Wongnawa, Triblock copolymer-templated synthesis of porous TiO_2 and its photocatalytic activity, J. Nanopart Res. 12 (2010) 2895–2906.

[20] N. Sobana, M. Muruganadham, M. Swaminathan, Nano-Ag particles doped TiO_2 for efficient photodegradation of direct azo dyes, J. Mol. Catal. A: Chem. 258 (2006) 124–132.

[21] S. Anandan, P.S. Kumar, N. Pugazhenthiran, J. Madhavan, P. Maruthamuthu, Effect of loaded silver nanoparticles on TiO_2 for photocatalytic degradation of Acid Red 88, Sol. Energy Mater. Sol. Cells 92 (2008) 929–937.

[22] I.K. Konstantinou, T.A. Albanis, TiO_2-assisted photocatalytic degradation of azo dyes in aqueous solution: kinetic and mechanistic investigations, Appl. Catal. B: Environ. 49 (2004) 1–14.

[23] B. Wen, C. Liu, Y. Liu, optimization of the preparation methods synthesis of meso structures TiO_2 with high photocatalytic activities, J. Photochem. Photobiol. A: Chem. 173 (2005) 7–12.